A Journal of the Gesellschaft Deutscher Chemiker

Angewandte International Edition GDCh Chemie

www.angewandte.org

## Accepted Article

**Title:** Discovery and Mechanistic Elucidation of NQO1-Bioactivatable Small Molecules That Overcome Resistance to Degraders

**Authors:** Bárbara MG. Barbosa, Aikaterini Sfyaki, Sergi Rafael, Ferran José-Duran, Joan Pous, Carolina Sánchez-Zarzalejo, Carles Perez-Lopez, Mar Vilanova, Marko Cigler, Marina Gay, Marta Vilaseca, Georg E. Winter, Antoni Riera, and Cristina Mayor-Ruiz



**To be cited as:** *Angew. Chem. Int. Ed.* **2023**, e202316730

**Link to VoR:** https://doi.org/10.1002/anie.202316730

WILEY VCH

# Discovery and Mechanistic Elucidation of NQO1-Bioactivatable Small Molecules That Overcome Resistance to Degraders

Bárbara MG. Barbosa[1,+], Aikaterini Sfyaki[1,+], Sergi Rafael[1,+], Ferran José-Duran[1], Joan Pous[1], Carolina Sánchez-Zarzalejo[1], Carles Perez-Lopez[1], Mar Vilanova[1], Marko Cigler[2], Marina Gay[1], Marta Vilaseca[1], Georg E. Winter[2], Antoni Riera[1,3,*], and Cristina Mayor-Ruiz[1,*]

[1] Institute for Research in Biomedicine (IRB Barcelona), the Barcelona Institute of Science and Technology (BIST), 08028 Barcelona, Spain
[2] Research Center for Molecular Medicine of the Austrian Academy of Sciences (CeMM), 1090 Vienna, Austria
[3] Departament de Química Inorgànica i Orgànica, Secció Química Orgànica, Universitat de Barcelona, Martí i Franquès 1, 08028 Barcelona, Spain

[+] These authors contributed equally
* Corresponding authors: antoni.riera@irbbarcelona.org and cristina.mayor-ruiz@irbbarcelona.org

## ABSTRACT

Degraders hold the promise to efficiently inactivate previously intractable disease-relevant targets. Unlike traditional inhibitors, degraders act substoichiometrically and rely on the hijacked proteolysis machinery, which can also act as an entry point for resistance. To fully harness the potential of targeted protein degradation, it is crucial to comprehend resistance mechanisms and formulate effective strategies to overcome them. We conducted a chemical screening to identify synthetic lethal vulnerabilities of cancer cells that exhibit widespread resistance to degraders. Comparative profiling followed by tailored optimization delivered the small molecule RBS-10, which shows preferential cytotoxicity against cells pan-resistant to degraders. Multiomics deconvolution of the mechanism of action revealed that RBS-10 acts as a prodrug bioactivated by the oxidoreductase enzyme NQO1, which is highly overexpressed in our resistance models. Collectively, our work informs on NQO1 as an actionable vulnerability to overcome resistance to degraders and as a biomarker to selectively exploit bioactivatable prodrugs in cancer.

## INTRODUCTION

Targeted protein degradation (TPD) is a pharmacological modality that induces the elimination of proteins by hijacking one of the cell's natural protein removal systems. To date, most work on TPD has focused on the chemical rewiring of the ubiquitin–proteasome system. Mechanistically, TPD is based on small-molecule "degraders" that induce proximity between a protein of interest and an E3 ubiquitin ligase, leading to the polyubiquitination and consequent proteasomal degradation of the former.[1-5] This strategy has garnered significant attention in recent years, especially owing to its potential to inactivate previously intractable drug targets. Beyond the interest of TPD as a therapeutic approach, degraders are broadly used in research settings to evaluate the acute consequences that accompany the removal of a given protein. Degraders can be monovalent (e.g., molecular glue degraders) or multivalent (e.g., PROTACs), depending on whether they are composed by one ligand or by more than one (typically two) linked ligands.[5-6] Clinical proof of concept for TPD is provided by the anti-myeloma drug lenalidomide and related immunomodulatory imide drugs (IMiDs). IMiDs are molecular glue degraders that hijack the E3 ligase $CRL4^{CRBN}$ to deplete a range of proteins, including the transcription factors IKZF1/3.[7-12] Several degraders are currently being tested in clinical trials.[4]

Most of the degraders available hijack E3s of the cullin RING ligase (CRL) superfamily. CRLs are multisubunit dynamic complexes nucleated by a core consisting of a cullin scaffold (CUL1-9) and its dedicated RBX partner (RBX1 or RBX2). Ubiquitination depends on >200 substrate receptors (SRs) that each recognize specific protein substrates. SRs bind interchangeably with a particular CRL core, either directly or via adaptors, and are the defining component of the specific subfamily complex ($CRL^{SR}$).[13-15] Degraders typically function by hijacking SRs such as CRBN ($CRL4^{CRBN}$), VHL ($CRL2^{VHL}$), or DCAF15 ($CRL4^{DCAF15}$). CRL plasticity and physiological impact depend on coordinated interactions with positive and negative regulators (e.g., neddylation enzymes, the COP9 signalosome, and CAND1).[16-17]

TPD relies on multiple components, namely E3- and target-related constituents, thus several opportunities for the development of resistance may arise. A unique feature of degraders is that they act substoichiometrically: after target elimination, a degrader can induce the ubiquitination of another target molecule. Conceivably, the hijacked proteolysis machinery needs to sustain such a catalytic process, which in turn can act as an additional (or alternative) entry point for resistance. Indeed, functional genomic campaigns in recent years have helped map how the repertoire of CRLs and their regulators shape degrader efficacy and resistance.[3, 18-29] We and others have conducted CRISPR-based screens to show that resistance to degraders is predominantly defined by the nature of the hijacked CRL and not by the degraded target. These unique mechanisms differ from the target-centric resistance associated with traditional inhibitors and mainly involve the loss of one of the following: (a) the hijacked SR or other CRL components, (b) the implicated E2 ubiquitin-conjugating enzymes, or (c) key negative/positive CRL regulators.[3] UBE2M, a neddylation E2-conjugating enzyme involved in CRL activation, is the only reported example whose loss of function confers cross-resistance to all the available CRL-based degraders.[3, 30] In addition to CRISPR screens, constant exposure to degraders coupled with SR mutagenesis has recently highlighted residues at the E3 interface prone to cause resistance to some degraders.[27] There are also examples of target-driven resistance to degraders via point mutations.[28-29] The growing body of data in cellular models will continue to enlighten potential resistance mechanisms to degraders in the clinic.

Here, we set out to identify synthetic lethal vulnerabilities of cancer cells that show widespread resistance to degraders, namely: UBE2M mutant ($UBE2M^{mut}$) cells. Target-agnostic comparative chemical profiling of a drug library (4,000 compounds) yielded a drug hit with preferential cytotoxicity against $UBE2M^{mut}$ cells. An orthogonal target deconvolution campaign allowed us to elucidate the mechanism of action of the optimized analog RBS-10. We discovered that RBS-10 is a prodrug activated by the NAD(P)H:quinone oxidoreductase 1 (NQO1)[31] and whose metabolites generate reactive oxygen species (ROS) leading to DNA damage and apoptosis. Mechanistically, we showed that inactivation of $CRL3^{KEAP1}$ leads to NQO1 upregulation. Thus, we have discovered an actionable vulnerability to fight degrader resistance mechanisms that lead to CUL3 (or KEAP1) inactivation. In addition, we demonstrate the ability of NQO1-bioactivatable clinical compounds, such as mitomycin C, to overcome widespread resistance to degraders, thereby offering a plausible path to deal with this type of resistance mechanisms in the clinic. Finally, we studied the use of RBS-10 in cancer beyond degrader resistance since NQO1 is highly expressed in many solid tumors,

including lung and breast cancer.[32] We showed that NQO1 levels are a biomarker of sensitivity to RBS-10 in breast cancer. Taking all together, our findings inform on synthetic lethal interactions to overcome promiscuous resistance to degraders and reaffirms the use of high NQO1 levels as a way to selectively exploit redox-activated prodrugs in particular types of cancer.

## RESULTS AND DISCUSSION

### Synthetic lethal drug screens to overcome pan-resistance to degraders

Conceptually, the loss of function of a broad CRL regulator poses an advantageous mechanism to evade the action of a wide range of degraders. Indeed, UBE2M$^{mut}$ cells showed universal resistance to CRL-based degraders independent of the co-opted SR[3, 30]. We previously reported that such broad resistance is due to promiscuous CRL hyponeddylation and, thus, impairment of the CRL activity.[3, 30].

In brief, UBE2M loss could offer a significant advantage to degrader-treated cancer cells, particularly in scenarios where agents against the same target but recruiting different E3 ligases may be administered. This approach is currently considered a potential means to counteract resistance to PROTACs (over 15 of which are presently undergoing clinical trials). Indeed, UBE2M$^{mut}$ cells were resistant to degraders against the same target (BRD4) but recruiting different E3s (CRBN or VHL), administered either as single agents or concomitantly (**Figure S1A**). Alternative strategies are needed to overcome resistance to degraders caused by the loss of broad E3 regulators. Importantly, UBE2M deficiency also confers resistance to newer generations of degraders that co-opt the lysosomal degradation machinery (lysosome-targeting chimeras –LYTACs).[33]

Here, we set out to identify the synthetic lethal dependencies of UBE2M$^{mut}$ as a proxy to tackle resistance to degraders. Inspired by our previous experience with differential chemical profiling, we conducted a new target-agnostic drug screen based on differential viability. Wild-type (WT) and UBE2M$^{mut}$ KBM7 cells were treated with a library of around 4,000 prioritized small molecules (cytotoxic/cytostatic in WT cells) at 2 doses, and viability was measured 3 days later. A total of 370 molecules were prioritized for a secondary dose-resolved screening at 8 doses per compound, yielding 5 hits that preferentially affected the fitness of UBE2M$^{mut}$ cells (**Figure 1A**). Dose-ranging validations led us to select RBS-1 for further optimization and mechanistic evaluation (**Figure 1B,C**).

We conducted a structure-activity-relationship (SAR) study (**Figure 1D,E** and **S1B**). We first observed that only the compound containing the terminal 2-nitrofuran fragment exhibited cellular toxicity (RBS-1 vs. RBS-2 to 5). We next improved the substitution in the central ring by changing it from *meta* (RBS-7) to *para* (RBS-10). The 3-methylbenzamide fragment gave the best results (RBS-10 vs. RBS-17, 18 and 20). The substitution of the nitro group for other structurally similar electron-withdrawing groups such as sulfonyl, trifluoromethyl or carboxylic acids (RBS-11 to 16) showed a loss of the activity and selectivity towards UBE2M$^{mut}$ cells. RBS-10 was the most potent and UBE2M$^{mut}$–selective analog of the SAR studies (**Figure 1E-G**), which was confirmed in an additional UBE2M$^{mut}$ model (**Figure S1C**). Of note, the minimal change of the substitution of the furan ring by a thiophene (RBS-10 to

10.1002/anie.202316730

RBS-11) resulted in a significant loss of potency and selectivity. Further derivatization of the terminal methyl group in RBS-10 (RBS-21 to 22) did not improve the results obtained with RBS-10 (**Figure 1D-G** and **S1B**). In summary, comparative chemical profiling and subsequent chemical optimization led to the discovery of RBS-10, a small molecule that can tackle pan-resistance to degraders.

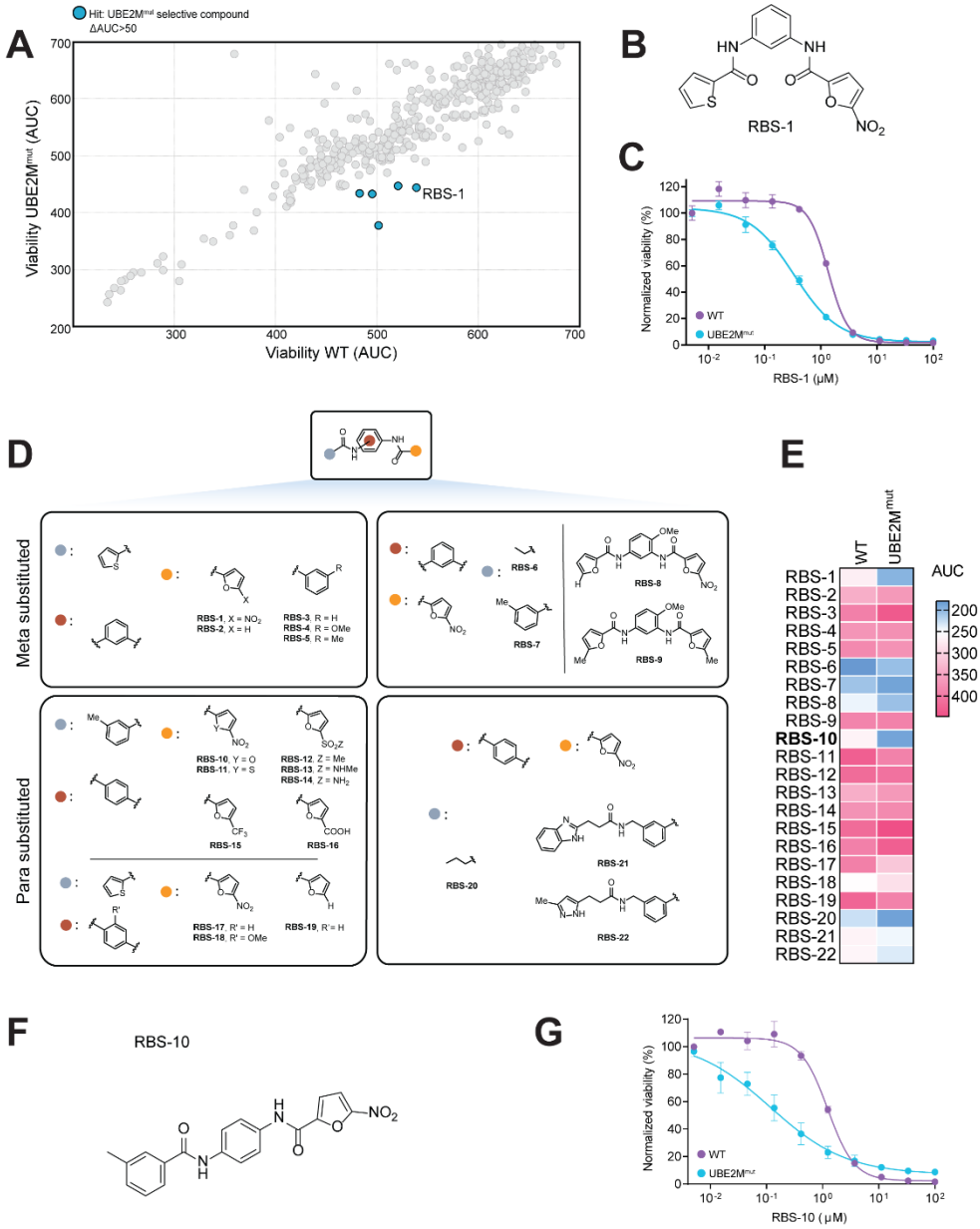


***Figure 1**. Synthetic lethal drug screening and SAR studies identify compound RBS-10 as preferentially cytotoxic in models pan-resistant to degraders. (A) Drug screen with the 370 prioritized small molecules. In blue, compounds that preferentially affect the viability of UBE2M$^{mut}$ vs. WT cells (threshold for hit calling: ΔAUC>50). (B) RBS-1 chemical structure. (C) Dose-resolved DMSO-normalized viability after 3 days of RBS-1 treatment in the indicated genetic backgrounds of KBM7 cells. Mean ± SEM; n = 3 independent treatments.(D) Analogs of RBS-1 evaluated in the SAR study.(E) Heatmap depicting results of the SAR study based on differential cell viability (UBE2M$^{mut}$ vs. WT cells). Results are represented as relative area under the curve (AUC) calculated from dose-resolved DMSO-normalized viability after 3 days of compound treatment. (F) Chemical structure of RBS-10, the best chemical analog of the SAR studies. (G) Dose-resolved DMSO-normalized viability after 3 days of RBS-10 treatment in the indicated genetic backgrounds of KBM7 cells. Mean ± SEM; n = 3 independent treatments*

## Target identification and validation of RBS-10

Next, we dissected the mechanism of action of RBS-10 via multiomics target deconvolution. Target identification was initially conducted through chemoproteomic studies using RBS-$10_{NH2}$, a tethered RBS-10 analog. Based on our SAR study (**Figure 1D-G** and **S1A**), we determined that the methyl group of the 3-methylbenzamide fragment on RBS-10 was the optimal site for further derivatization. The addition of a free amine to this site did not disrupt RBS-10 activity (**Figure 2A** and **S2A**). RBS-$10_{NH2}$ allowed immobilization of the drug on sepharose beads and purification of interacting proteins from whole-cell lysates (**Figure 2A**). Coupling drug-affinity chromatography pulldowns with proteomics in a competitive setup (**Figure 2A** and **S2B**) revealed a very clear enrichment in one drug-interacting protein, **NQO1**, an NAD(P)H quinone oxidoreductase enzyme (**Figure 2B** and **Supplementary Table 1**).[31-32] NQO1 catalyzes the two-electron reduction of quinones and a range of xenobiotics. NQO1 works through a “ping-pong” mechanism, whereby the tightly bound cofactor flavin adenine dinucleotide (FAD) is first reduced by NAD(P)H. The oxidized form (NAD(P)+) then leaves the active site, thereby enabling the quinone (or alternative substrate) to enter and be readily reduced by $FADH_2$.[34] NQO1 functions as a homodimer[35] and its frequent overexpression in cancer makes it an attractive therapeutic target.[31-32] Interestingly, we observed a striking overexpression of NQO1 in UBE2M$^{mut}$ cells compared to WT KBM7 cells (**Figure 2C**), an observation that was extended to other cancer models in which we genetically or chemically impaired UBE2M function (**Figure S2C,D**). We confirmed NQO1 binding to RBS-10 both in intact cells (using thermal shift assays) (**Figure 2D**), and in vitro (via microscale thermophoresis) (**Figure S2E**). Additionally, we observed that RBS-10 inhibited the enzymatic activity of NQO1, again in intact cells and in vitro (**Figure 2E** and **S2F**). The known NQO1 inhibitors dicoumarol[36] and ES936[37] were included as positive controls.

## Structural characterization of RBS-10 bound to NQO1

Finally, the crystallization of RBS-10 bound to human NQO1, showed that RBS-10 engages NQO1 at the active site (**Figure 2F**). Our crystal structure revealed two NQO1 monomers that generate a stable protein-protein interface where the two catalytic pockets coexist at opposite sides of the dimer. The electron density of the cofactor FAD is observed in one of the active sites, whereas RBS-10 appears in the second pocket (**Figure 2F**). Docking studies helped us map the key protein-ligand interactions. The most energetically favourable poses repeatedly presented the nitrofuran group from RBS-10 buried in the deepest region of the NQO1 active site, with the nitro group hydrogen-bonded with Tyr155, Phe106, and Leu103 (**Figure 2G**). Interestingly, the NQO1 residue Phe106 is relevant in the binding of most reported inhibitors.[36-38] In brief, our orthogonal target deconvolution campaign nominated RBS-10 as an inhibitor of NQO1. Collectively, these data provided a hypothesis for the observed preferential efficacy of RBS-10 in UBE2M$^{mut}$ cells: NQO1 expression was exacerbated in this model pan-resistant to degraders and, hence, the loss of NQO1 activity may represent an actionable dependency.

10.1002/anie.202316730

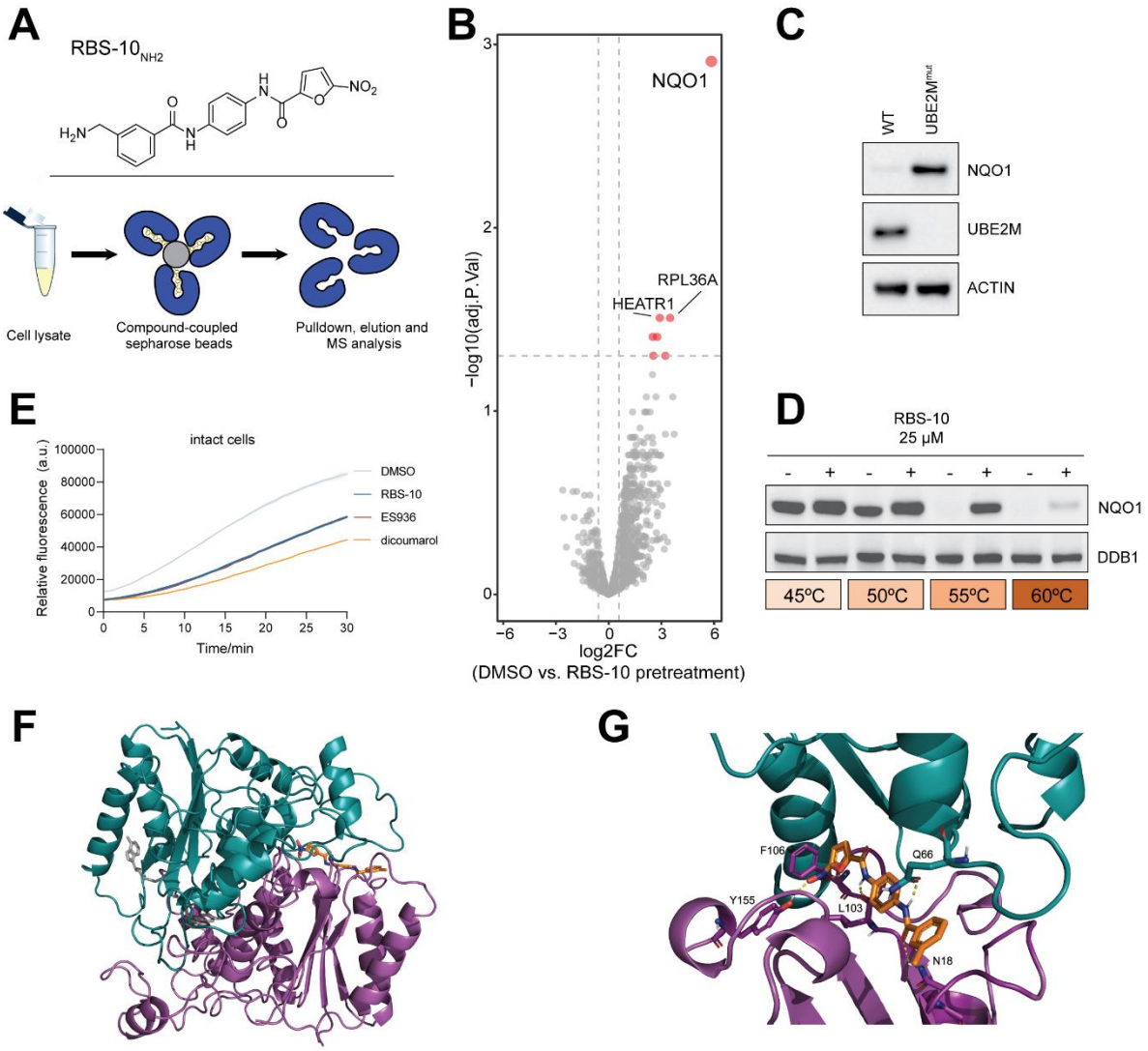


***Figure 2.*** *Chemoproteomics reveals NQO1 as a target of RBS-10. (A) Structure of the probe RBS-10$_{NH2}$ and schematics of the chemoproteomics approach. (B) Chemoproteomics results after 2 h of treatment with RBS-10$_{NH2}$-coupled beads in lysates pre-treated with DMSO or RBS-10 for 1 h (competition setup, see also Extended Data Figure 2a) in WT cells. (C) NQO1 protein levels in WT vs. UBE2M$^{mut}$ KBM7 cells. (D) Endogenous NQO1 levels in UBE2M$^{mut}$ KBM7 cells upon thermal destabilization after DMSO or RBS-10 (25 µM) treatment for 2 hours. Representative image of 5 independent experiments. (E) Time-resolved DMSO-normalized NQO1 activity assay based on the fluorescently-labeled quinone substrate QL.MU[39] in intact KBM7 cells (RBS-10, dicoumarol, and ES936 25 µM). Representative of 3 independent experiments. (F) New X-ray crystal structure (3.8 Å) of NQO1 bound to RBS-10 (PDB:8PQN). Co-crystallization: NQO1, FAD, and RBS-10, in the absence of NAD(P)H. Top monomer of NQO1 is shown in green and bottom one in magenta, cofactor FAD in gray, and RBS-10 in orange.(G) Molecular docking of RBS-10 in NQO1 (PDB:5EA2 used for better resolution). Key interactions are shown in dashed yellow lines, and the NQO1 residues involved are highlighted. Uncropped blots for Fig.2 are in the Supporting Information.*

## NQO1 activity is indispensable for the mechanism of action of RBS-10

To explore whether the inhibition of NQO1 activity mediated the preferential deleterious effect of RBS-10 in UBE2M$^{mut}$ vs. WT cells, we assessed the essentiality of NQO1 in both cellular backgrounds. CRISPR-based gene disruption experiments showed that NQO1 deletion prompted no measurable fitness defect in UBE2M$^{mut}$ cells (or WT cells) (**Figure 3A,B**). This observation is in agreement with genome-scale CRISPR/Cas9 screening data

10.1002/anie.202316730

that is publicly available in DepMap.org[40], where NQO1 lacks an essential profile in the >1,000 cancer cell lines included (**Figure S3A**).[41]

To map the cellular effectors required for RBS-10 activity, we conducted genome-wide CRISPR screens of resistance. sgRNAs targeting *NQO1* and *NEF2L2* (the latter encoding for NRF2, key transcriptional activator of NQO1 expression) scored as the top genetic determinants (**Figure 3C** and **Supplementary Table 2**). Hence, our data implies that NQO1 is indeed required for RBS-10 cytotoxic activity (**Figure 3C,D**). sgRNAs targeting *GSTO1* and *ARNT* were the other top hits in the CRISPR screen. The deficiency of these proteins is mechanistically linked to NQO1 depletion. *Gsto1*$^{-/-}$ mice have lower expression of NQO1[42] and reduction of ARNT dramatically represses NQO1 expression.[43] Interestingly, well-known inhibitors of NQO1 did not show selective cytotoxicity against our model of pan-resistance to degraders (**Figure S3B,C**). All these findings highlighted the distinct mechanism of action of RBS-10, setting it apart from these inhibitors.

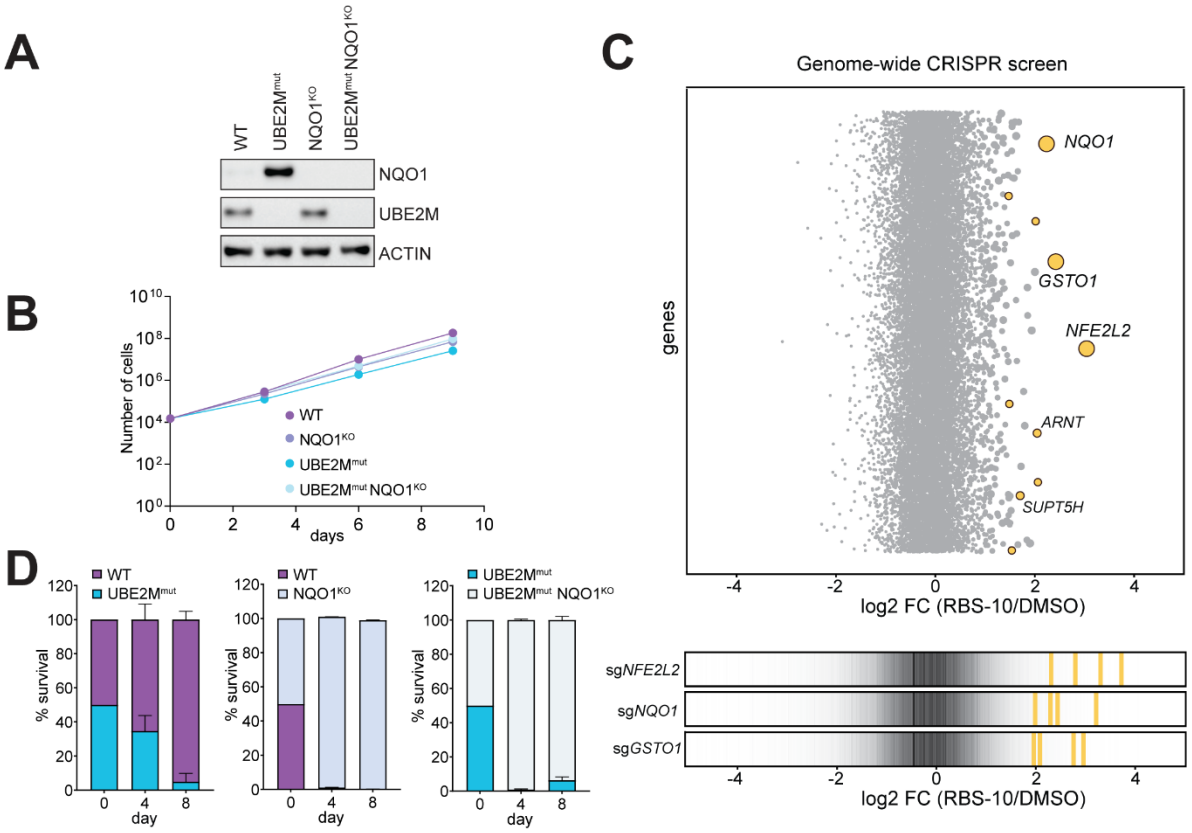


***Figure 3**. The mechanism of action of RBS-10 requires NQO1 activity. (A) NQO1 protein levels in KBM7 clones with the indicated genetic background (WT or UBE2M$^{mut}$) generated with CRISPR/Cas9. Uncropped blot in the Supporting Information. (B) Growth curves in the indicated genetic backgrounds show that NQO1 is not essential. (C) Genome-wide CRISPR screens of resistance to RBS-10. Top: bubble plot displaying median sgRNA enrichment over DMSO, bubble size indicates significance. Bottom: sgRNA enrichment targeting indicated genes, background in gray indicates the distribution of all sgRNAs. The top-2 genes in sgRNA enrichment were NQO1 and NFE2L2 (the latter encoding for NRF2, a key transcriptional activator of NQO1 expression). (D) DMSO-normalized competition growth experiments. The indicated genetic backgrounds of KBM7 cells were mixed at 1:1 ratio (dTomato- and eGFP-expressing cells per comparison), treated with RBS-10 (0.9 μM) and flow cytometry quantified at days 0, 4, and 8. Mean ± SEM; n = 3 independent treatments.*

## RBS-10 is a prodrug metabolized by NQO1

We hypothesized that RBS-10 could be a prodrug that needs to be bioactivated by NQO1 to exert its cytotoxic effect. Several compounds, although mostly quinones, require bioreduction by NQO1 to have antitumor activity[31]. As NQO1 is highly expressed in many solid tumors, bioactivatable prodrugs have become increasingly attractive. To explore this model, we conducted proteomic studies with recombinant NQO1. Intact LC-MS denaturing analysis (Orbitrap Fusion Lumos instrument) with NQO1, the cofactor FAD and the hydrogen donor NADPH, incubated with RBS-10 for 1 h, did not reveal any NQO1 adduct nor did LC-MS/MS experiments with NQO1 digested with trypsin or chymotrypsin. We could therefore disregard the possibility of an irreversible covalent interaction between NQO1 and RBS-10 or its potential metabolites. Preliminary control studies in native conditions (Synapt G1 HDMS instrument) showed that NQO1 is a dimer that includes the FAD cofactor, as previously reported.[44] The main ions detected in the control corresponded to 2NQO1 + 2FAD (m/z 3957, z = 16 and m/z 3724, z = 17). Native MS detected additional peaks pointing to NQO1 dimeric species with two FADs and one and two units of potential RBS-10 drug metabolites (+320-350 Da and +2x(320-350) Da, approximately). The interaction of NQO1 with these metabolites is strong, as reflected by the trap voltages used to disrupt non-covalent complexes in the gas phase (> 90 V). However, the MS resolution in the Synapt G1 instrument was not enough to calculate an accurate mass for these metabolites (320 to 350 Da). To improve the resolution, we repeated the MS experiment in native conditions using an Orbitrap Eclipse mass spectrometer tuned to detect non-covalent interactions. The results of this study confirmed the formation of several RBS-10 metabolites. Samples containing different concentrations of RBS-10 (25 μM and 100 μM) showed the formation of the same species as in the control and a number of additional ions (**Figure 4A,B** and **S4A-C**). The resolution limit did not allow for distinguishing between structures that vary by 2 Da units given that the mass numbers are affected by the large ionization numbers. Nevertheless, on the basis of the approximate masses together and chemical reasoning, 367, 349 and 351 Da were the postulated molecular weights of the three main metabolites. In more detail, the peaks at m/z 3746.4 (z=17) and m/z 3980.4 (z=16) were associated to 2NQO1+2FAD+(366-369) Da. Peaks at 3745.4 (z=17) and 3979.2 (z=16) were associated to 2NQO1+2FAD+(347-349) Da. Peaks at m/z 3765.6 (z=17) and m/z 4000.8 (z=16) were associated to 2NQO1+2FAD+2(344-350) Da. Finally, the peaks at 3699.1 (z=17) and 3930.4 (z=16) were associated to 2NQO1+1FAD+(346-347) Da (**Figure 4A,B** and **S4A-C**).

To gain further insight into the nature of the metabolites, an LC/MS/MS study was undertaken. Three main peaks were observed with the following m/z: 350, 352 and 368 Da, in great agreement with the native MS results. Given that the molecular weight of RBS-10 is 365 Da, the m/z of 350 Da could be assigned to the $[M+H]^+$ of the nitroso compound RBS-10M1 (**Figure 4C**). The reduction of RBS-10M1 to the hydroxylamine RBS-10M2 would give the expected mass of 352 for the $[M+H]^+$ cation (**Figure 4C**). These two metabolites are in agreement with previous precedents.[44] The peak of 368 Da corresponds to the addition of water to RBS-10M1. The addition of water to a furan ring is well known, for instance in the metabolism of Nifurtimox.[44] Several structures can be hypothesized that would account for this metabolite. However, the MS/MS spectra, with a loss of OH, NH and CO (**Figure S4D**) led us to postulate RBS-10M3 as the most feasible (**Figure 4C**).

10.1002/anie.202316730

We attempted several strategies to synthesize the elucidated metabolites but all were unsuccessful, since, as previously reported, amino furans are highly unstable and cannot be isolated.[45-46] Nevertheless, our orthogonal elucidation of these metabolites by intact proteomics and metabolomics is also supported by literature precedents about the mechanism of the reduction of the nitrofuran moiety.[47-48] Together with the genetic rescue of RBS-10 cytotoxicity observed in NQO1$^{KO}$ cells, these data supports its prodrug nature.

To further corroborate the prodrug mechanism of action of RBS-10, our prior crystallization results (**Figure 2F**) encouraged us to attempt the structural characterization of the NQO1-bound metabolite(s). Unfortunately, no protein crystals grew in the presence of the electron donor NADPH. Nevertheless, molecular docking allowed us to unveil potential key interactions of the most plausible metabolite RBS-10M3 (**Figure 4D**). The docking results showed that this metabolite shares important binding features with the parental molecule RBS-10 (**Figure 2G** and **Figure 4D**): (1) it engages the same catalytic pocket, and (2) the opened nitrofuran group points towards the buried cavity. In addition, RBS-10M3 is predicted to interact with the FAD cofactor, and two NQO1 residues: Trp105 and Tyr126. Interestingly, Tyr126 is critical for NQO1 catalytic activity (**Figure 4D**). [36-38] The best binding energy poses were obtained with (*E*)-RBS-10M3.

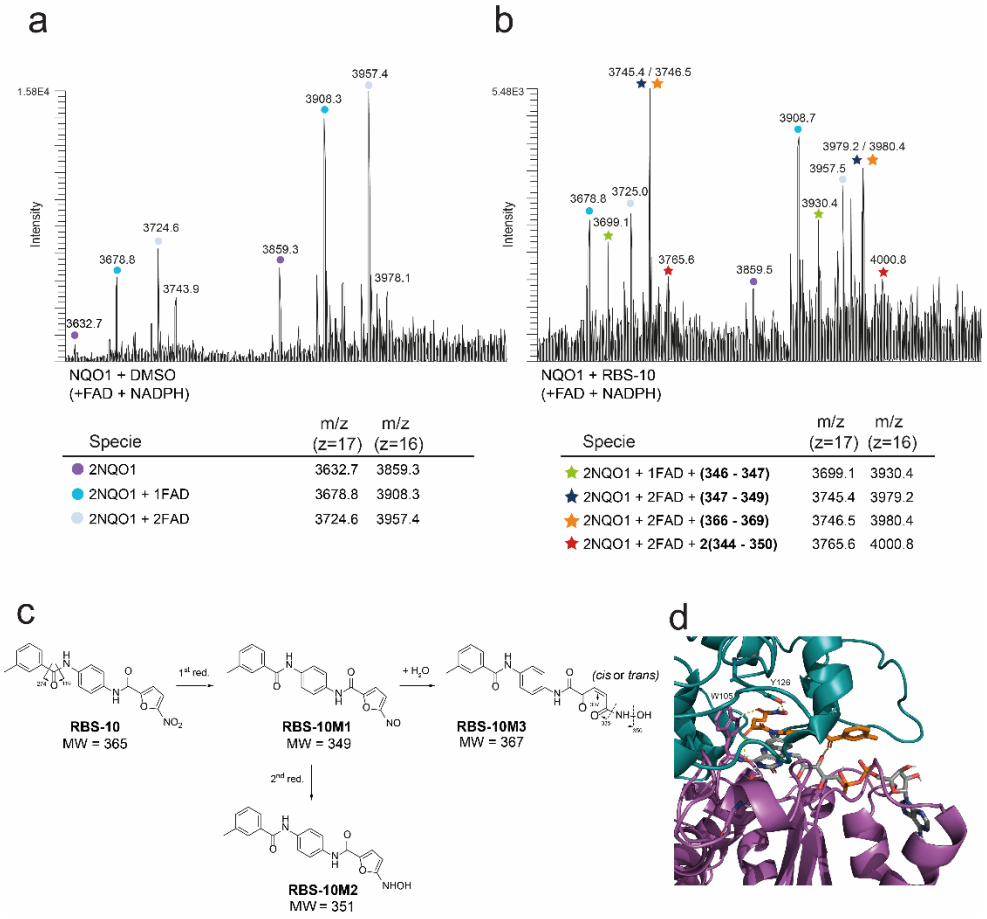


***Figure 4.*** *RBS-10 is a prodrug bioactivated by NQO1. (A,B) Selected MS spectra from the native proteomics studies (Orbitrap Eclipse mass spectrometer). (A) Recombinant NQO1 + FAD + NADPH without the addition of RBS-10 and (B) incubated with 100 μM of RBS-10. (C) Proposed structures for the metabolites of RBS-10 based on intact proteomics and metabolomics. Units: Da. (D) Molecular docking of (E)-RBS-10M3 in the NQO1 homodimer (PDB:5EA2 used for better resolution) in the presence of the cofactor FAD. Top monomer of NQO1 is shown in green, bottom one in magenta, RBS-10M3 in orange, and FAD in grey. Key interactions are shown in dashed yellow lines, and the NQO1 residues involved are highlighted.*

10.1002/anie.202316730

## RBS-10 bioactivation by NQO1 induces ROS and DNA damage

Next, we focused on the molecular mechanisms driving the cytotoxic effect of RBS-10 metabolism. We observed NQO1-dependent induction of ROS upon treatment with RBS-10 (**Figure 5A,B**), leading to DNA damage (**Figure 5C,D** and **S5A**), and apoptosis (**Figure 5E** and **S5B**). In all cases, these effects were rescued in the absence of NQO1 (**Figure 5A-E**). Glutathione (GSH) is one of the major cellular antioxidants. Under pro-oxidant conditions, two GSH molecules donate one electron each and are converted to glutathione disulfide (GSSG). The reduced-to-oxidized glutathione ratio (GSH/GSSG) is considered a powerful index of oxidative stress. On the basis of our GSH/GSSG experiments (**Figure 5B**), we hypothesize that some metabolites of RBS-10 are reduced by GSH[49], perhaps mainly mediated by the GSH transferase GSTO1, whose depletion was a top hit in our CRISPR screens (**Figure 3C**). Moreover, a conjugate addition of GSH to metabolites such as RBS-10M3 might take place and evolve increasing ROS and DNA damage.[50] Interestingly, NQO1 expression is induced as a part of the NRF2-directed response to cellular oxidative stress[51]. RBS-10 treatment also prompts NQO1 overexpression (**Figure S5B**), which can indeed contribute to an augmented cytotoxic effect caused by the concomitant intensification of the NQO1-mediated bioactivation of RBS-10. Collectively, intact proteomics, metabolomics and molecular docking confirmed the NQO1-mediated metabolism and activation of RBS-10, which in turn lead to ROS, DNA damage, and apoptosis in cells with high levels of NQO1.

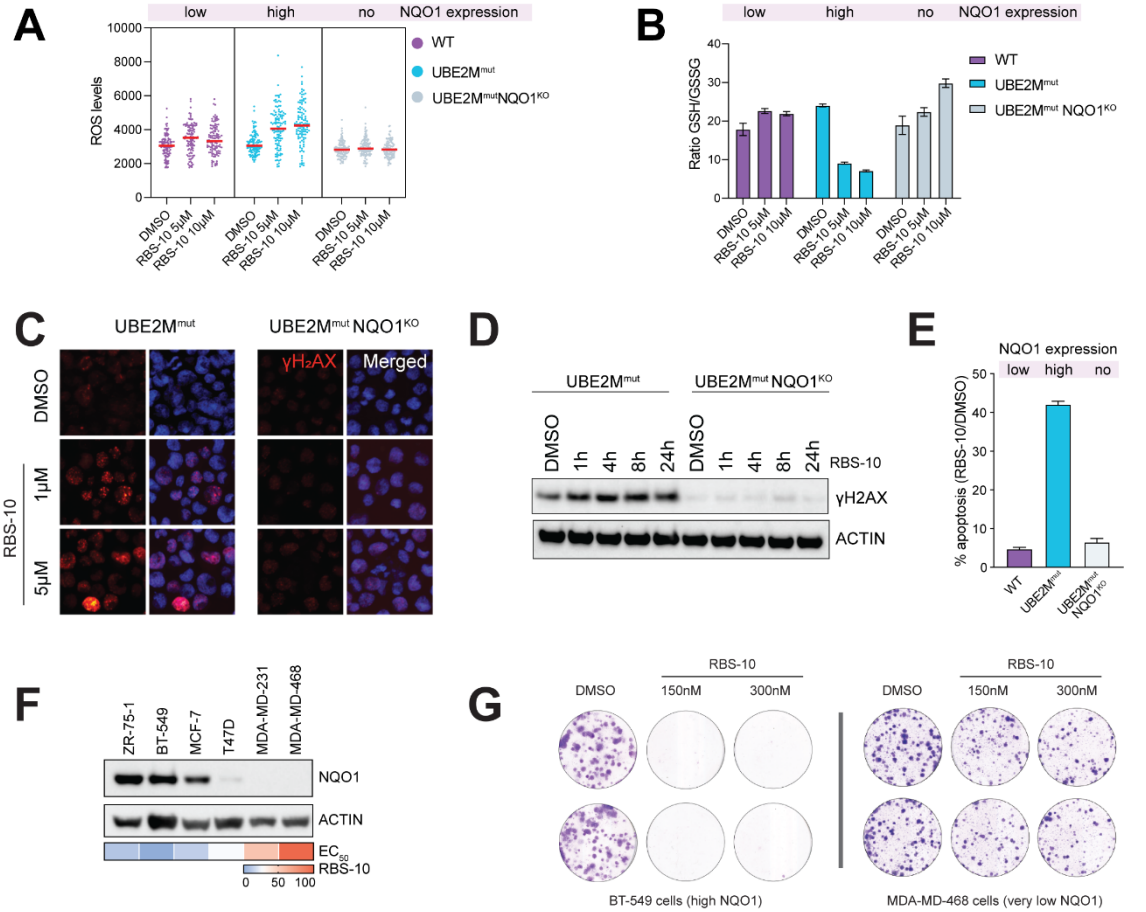


***Figure 5.*** *NQO1 levels as a biomarker of sensitivity to RBS-10. (A) Intracellular ROS generation measured via live confocal microscopy using 5 μM CellROX Deep Red fluorogenic probe in the indicated genetic backgrounds of KBM7 cells upon DMSO or RBS-10 treatment (24h at the indicated doses). Dots: Deep Red intensity per cell.*

*Medians are shown in red. (B) The GSH/GSSG ratio (index of oxidative stress) was determined in the indicated genetic backgrounds of KBM7 cell treated with DMSO or RBS-10 for 24h at the indicated doses. Mean ± SEM.; n = 3 independent treatments. (C) Representative images of UBE2M$^{mut}$ (high NQO1 levels) vs. UBE2M$^{mut}$ NQO1$^{KO}$ cells exposed to RBS-10 for 48h at the indicated doses. γH2AX in red, DAPI in blue. See Extended Data Figure 5a for quantification. (D) γH2AX levels upon time-resolved treatment with 5 μM RBS-10 UBE2M$^{mut}$ (high NQO1 levels) vs. UBE2M$^{mut}$ NQO1$^{KO}$ cells. (E) Apoptosis induction assessed by flow cytometry after staining with AnnexinV/propidium iodide (PI) in KBM7 cells treated with DMSO or RBS-10 (5 μM, 24 h). Representative of 3 independent experiments. Gating: FSC/SSC; singlets; AnnexinV/PI +. (F)* NQO1 protein levels in different cell lines of breast cancer. Bottom: *Heatmap with the RBS-10 EC50 values in the indicated breast cancer cell lines (see Figure S5F for viability curves). NQO1 levels correlate with sensitivity to RBS-10. (G) Colony formation assay in NQO1 high vs. low breast cancer cells at the indicated RBS-10 doses. Uncropped blots for Fig.5 are in the Supporting Information.*

## NQO1 levels as a biomarker of sensitivity to RBS-10

Finally, we explored the molecular mechanisms driving NQO1 overexpression in our cells with widespread resistance to degraders. Under steady-state conditions, the activity of NRF2, a major NQO1 transcriptional activator, is repressed by CRL3$^{KEAP1}$, which induces NRF2 ubiquitination and proteasomal degradation.[52] We previously showed that the broad resistance to degraders in the absence of UBE2M activity is due to promiscuous CRL hyponeddylation.[3, 30] Therefore, we hypothesized that NQO1 overexpression in UBE2M$^{mut}$ cells was caused by the inactivation of CRL3$^{KEAP1}$, which in turn would lead to NRF2-mediated NQO1 transcriptional (over-)activation (**Figure S5C**). Indeed, CUL3 hyponeddylation (inactivation) (**Figure S5D**) and transcriptional upregulation of NQO1 (**Figure S5E**) was observed. This is in line with our observations that NQO1 levels can be increased upon treatment with a preclinical neddylation inhibitor (**Figure S2D**). Therefore, these findings revealed an actionable vulnerability (NQO1 overexpression) to fight degrader resistance mechanisms that converge in CRL inactivation (CRL3/KEAP1 in particular).

The discovery and characterization of RBS-10 have taught us that pan-resistance to degraders can be tackled by exploiting the overexpression of NQO1 as an actionable vulnerability. This metabolic enzyme has a vital role in protecting cells against oxidative damage and electrophilic attack, and it is highly expressed in many solid tumors, suggesting a role in cancer development.[31, 53] Hence, we decided to test NQO1 levels as a biomarker of sensitivity to RBS-10. We focused on breast cancer given that high expression of NQO1 has been associated with tumor progression.[54] We observed that NQO1 levels correlated with sensitivity to RBS-10 (**Figure 5F,G** and **S5F**).

The nitrofuran structural component of RBS-10, which is typically a suboptimal feature from a medicinal chemistry perspective, makes it difficult to optimize this small molecule as a lead. However, the elucidation of its mechanism of action provided an exploitable liability for degrader-resistant cells and beyond. We tested the clinical compound mitomycin C, reported to be activated by NQO1[53, 55], and found that it can also overcome resistance to degraders. As RBS-10, mitomycin C preferentially killed NQO1-overexpressing cells (**Figure S5G**), thus offering a plausible strategy to tackle this type of resistance mechanism in the clinic.

In summary, our deconvolution of the mechanism of action of RBS-10 helped us find relevant synthetic lethal interactions to cope with widespread resistance to degraders and showcased the use of high NQO1 levels as means to exploit redox-activated prodrugs in

cancer.

## CONCLUSIONS

The TPD field is keeping a close eye on the PROTACs and molecular glue degraders currently in clinical trials. Lessons about the emergence of resistance in these clinical settings are expected to complement our current understanding of how cancer cells cope with degrader modalities. In this work, we used UBE2M$^{mut}$ cells as a model of broad resistance to degraders and leveraged target-agnostic chemical screening as a proxy to discover small molecules that help tackle degrader resistance. Interestingly, UBE2M deficiency not only confer resistance to degraders that co-opt the ubiquitin-proteasome system but also the lysosomal pathway.[33] Optimization of an initial drug hit led to the small molecule RBS-10. Through orthogonal deconvolution of its mechanism of action, our multiomics approach revealed that RBS-10 exerts its selective cytotoxicity through NQO1 bioactivation.

Our structural studies showed that RBS-10 engages the active site of NQO1 (**Figure 2F**). Crystal structures of several inhibitors bound to NQO1 (e.g., Dicoumarol, PDB:2F1O[36]; ES936, PDB:1KBQ[37]; E6a, PDB:5EAI[38]; MNPC, PDB:6LLC[56]; and AS1, PDB:3JSX[57]) share a similar binding conformation, in which the inhibitor engages with the isoalloxazine ring of the FAD cofactor through π-stacking interactions. Intriguingly, our crystallography studies revealed that the RBS-10 prodrug and FAD did not bind simultaneously within the catalytic pocket of any of the NQO1 monomers (**Figure 2F**). This observation suggests a dynamic and rapid interplay between RBS-10 and FAD at the same active site of NQO1, maybe difficult to capture in the crystals. Molecular docking also predicted key interactions between RBS-10 and the NQO1 residues Tyr155, Leu103, Gln66 and Asn18 (**Figure 2G**), reported to be involved in NQO1-FAD binding.[37-38, 56] Our docking studies with RBS-10 predicted an important interaction between the nitro group of the compound and Phe106, a residue that is relevant in the binding of most reported inhibitors.[36-38, 56] Remarkably, Tyr126, a residue repeatedly reported to be critical for the NQO1 catalytic activity, is predicted to interact with the RBS-10M3 metabolite (**Figure 4D**).[36-38, 56-57]

Mechanistically, RBS-10 metabolism induces apoptosis via ROS and DNA damage in an NQO1-dependent manner and this bioactivation is indispensable for the cytotoxic outcome (**Figure 3**). Based on our GSH/GSSG experiments (**Figure 5B**), it is reasonable to speculate that the RBS-10 metabolites undergo GSH-mediated reduction, possibly facilitated by GSTO1. Notably, the depletion of GSTO1 emerged as a prominent hit in our CRISPR screens (**Figure 3C**). Moreover, conjugate addition of GSH to metabolite RBS-10M3 might evolve increasing ROS and triggering DNA damage[50]. Further research is required to determine whether the resistance to RBS-10 observed in the absence of GSTO1 (**Figure 3C**) is attributed to the reported effect triggering NQO1 downregulation[42], to impaired transfer of GSH to the RBS-10 metabolites, or to a combination of both. Interestingly, we observed that RBS-10 treatment also leads to the overexpression of NQO1 (**Figure S5B**), as reported in the NRF2-orchestrated response to oxidative stress.[51] Such NQO1 overexpression triggered by RBS-10 could significantly contribute to an enhanced cytotoxic effect through the concurrent intensification of RBS-10 bioactivation. In addition, we showed

that NQO1 overexpression can be modulated with preclinical neddylation inhibitors (**Figure S2D**), revealing chemical means to potentiate the effect of NQO1-dependent prodrugs.

In summary, here we reveal an actionable vulnerability, namely NQO1 overexpression, which may help fight degrader resistance mechanisms related to CRL inactivation. Importantly, the initial comparative chemical screening was the key to uncovering this vulnerability, which would have not been identifiable through regular CRISPR synthetic lethality screening. Several small molecules with a degree of chemical analogy to RBS-10 have recently been reported and linked by some means to NQO1, in some cases as potential inhibitors.[56, 58-59] Our findings with RBS-10 support the study of the mechanistic role that NQO1 may play in facilitating the toxicity of those small molecules through redox-activation.

Given that NQO1 is highly expressed in many solid tumors, the design of anticancer agents activated by this enzyme, together with NQO1-targeted drug delivery, have been active areas of research.[60-61] Mitomycin C is a prime example of an NQO1-activatable antitumorigenic drug that is clinically approved[53, 55]. Similarly, EO9 and streptonigrin can be activated by NQO1-catalyzed reduction[62]. Our findings reaffirm and motivate translational investigation via the chemical probe RBS-10 and similar small molecules in cancer types with elevated NQO1 levels (e.g., tumors with upregulated NRF2 or with KEAP1 loss of function). Collectively, our results with RBS-10 endorse NQO1 as a therapeutically actionable dependency in cancer and to counteract mechanisms of resistance to degraders.

## SUPPLEMENTARY INFORMATION

The following data can be found in the Supporting Information:

(i) Supplementary figures S1−S5; (ii) Materials and Methods; (iii) Synthetic methods and characterization (PDF)

(iv) Supplementary Tables (Tables S1-S3) (XLSX)

## CONFLICT OF INTEREST

The authors declare the following competing financial interest(s): C.M.-R. is part of the SAB of Nostrum Biodiscovery. The C.M.-R. lab has received or receives research funding from Aelin Tx and Almirall. G.E.W. is scientific founder and shareholder of Proxygen and Solgate, and his lab received research funding from Pfizer. The rest of authors declare no competing financial interest.

## ACKNOWLEDGMENTS

We would like to thank the members of the Mayor-Ruiz lab and the Riera lab for helpful discussion that helped shape this work, especially J. Ward for valuable input in biophysical assays. We thank the Mass Spectrometry & Proteomics, the Advanced Digital Microscopy

(especially N. Giakoumakis), and the Functional Genomics core facilities at IRB Barcelona. We thank the Automated Crystallography Platform (IRB Barcelona, IBMB-CSIC) and the ALBA Synchrotron staff for support with the crystallization experiments and diffraction. We are grateful to A. Koren, S. Kubicek, and the CeMM Molecular Discovery Platform for their assistance with the chemical screening, and the URV-CIBERDEM-IIPSV Metabolomics Platform (especially to O. Yanes, A. Junza and J. Capellades). We apologize to those colleagues who could not be cited due to space limitations. The Mayor-Ruiz lab has funding from the European Research Council (ERC) as a Starting Grant to C.M-R. (ERC-2021-StG-101040046 TrickE3), "la Caixa" Foundation, FERO-ASEICA, AECC, the Mark Foundation for Cancer Research, the Spanish Ministry of Science and Innovation (PID2020-120110RA-I00; SMSI), and AGAUR-GenCat. The Riera's group has funding from FEDER/SMSI (PID2020-115074GB-I00) and AGAUR-GenCat (2021 SGR 00866). A. S. is supported by an FPI Severo Ochoa PhD fellowship (PRE2022-102653, SMSI), F.J-D. by an FPI PhD fellowship (PRE2021-098554, SMSI), and S.R. by an FI fellowship (2022FI_B1 00096, AGAUR-GenCat).

## REFERENCES

[1] A. C. Lai, C. M. Crews, *Nat Rev Drug Discov* **2017**, *16*, 101-114.
[2] E. Bulatov, A. Ciulli, *Biochem J* **2015**, *467*, 365-386.
[3] C. Mayor-Ruiz, M. G. Jaeger, S. Bauer, M. Brand, C. Sin, A. Hanzl, A. C. Mueller, J. Menche, G. E. Winter, *Mol Cell* **2019**, *75*, 849-858 e848.
[4] M. Bekes, D. R. Langley, C. M. Crews, *Nat Rev Drug Discov* **2022**, *21*, 181-200.
[5] A. Domostegui, L. Nieto-Barrado, C. Perez-Lopez, C. Mayor-Ruiz, *Chem Soc Rev* **2022**, *51*, 5498-5517.
[6] L. Nieto-Barrado, A. Domostegui, C. Mayor-Ruiz, in *Inducing Targeted Protein Degradation*, Wiley-Vch, **2023**, pp. 177-204.
[7] T. Ito, H. Ando, T. Suzuki, T. Ogura, K. Hotta, Y. Imamura, Y. Yamaguchi, H. Handa, *Science* **2010**, *327*, 1345-1350.
[8] J. Kronke, N. D. Udeshi, A. Narla, P. Grauman, S. N. Hurst, M. McConkey, T. Svinkina, D. Heckl, E. Comer, X. Li, C. Ciarlo, E. Hartman, N. Munshi, M. Schenone, S. L. Schreiber, S. A. Carr, B. L. Ebert, *Science* **2014**, *343*, 301-305.
[9] G. Lu, R. E. Middleton, H. Sun, M. Naniong, C. J. Ott, C. S. Mitsiades, K. K. Wong, J. E. Bradner, W. G. Kaelin, Jr., *Science* **2014**, *343*, 305-309.
[10] E. S. Fischer, K. Bohm, J. R. Lydeard, H. Yang, M. B. Stadler, S. Cavadini, J. Nagel, F. Serluca, V. Acker, G. M. Lingaraju, R. B. Tichkule, M. Schebesta, W. C. Forrester, M. Schirle, U. Hassiepen, J. Ottl, M. Hild, R. E. Beckwith, J. W. Harper, J. L. Jenkins, N. H. Thoma, *Nature* **2014**, *512*, 49-53.
[11] J. Kronke, E. C. Fink, P. W. Hollenbach, K. J. MacBeth, S. N. Hurst, N. D. Udeshi, P. P. Chamberlain, D. R. Mani, H. W. Man, A. K. Gandhi, T. Svinkina, R. K. Schneider, M. McConkey, M. Jaras, E. Griffiths, M. Wetzler, L. Bullinger, B. E. Cathers, S. A. Carr, R. Chopra, B. L. Ebert, *Nature* **2015**, *523*, 183-188.
[12] Q. L. Sievers, G. Petzold, R. D. Bunker, A. Renneville, M. Slabicki, B. J. Liddicoat, W. Abdulrahman, T. Mikkelsen, B. L. Ebert, N. H. Thoma, *Science* **2018**, *362*.
[13] T. Cardozo, M. Pagano, *Nat Rev Mol Cell Biol* **2004**, *5*, 739-751.
[14] J. R. Lydeard, B. A. Schulman, J. W. Harper, *EMBO Rep* **2013**, *14*, 1050-1061.
[15] M. D. Petroski, R. J. Deshaies, *Nat Rev Mol Cell Biol* **2005**, *6*, 9-20.
[16] R. J. Deshaies, *Annu Rev Cell Dev Biol* **1999**, *15*, 435-467.
[17] J. M. Reitsma, X. Liu, K. M. Reichermeier, A. Moradian, M. J. Sweredoski, S. Hess, R. J. Deshaies, *Cell* **2017**, *171*, 1326-1339.e1314.

[18] Q. L. Sievers, J. A. Gasser, G. S. Cowley, E. S. Fischer, B. L. Ebert, *Blood* **2018**, *132*, 1293-1303.
[19] G. Lu, S. Weng, M. Matyskiela, X. Zheng, W. Fang, S. Wood, C. Surka, R. Mizukoshi, C. C. Lu, D. Mendy, I. S. Jang, K. Wang, M. Marella, S. Couto, B. Cathers, J. Carmichael, P. Chamberlain, M. Rolfe, *Elife* **2018**, *7*.
[20] J. Liu, T. Song, W. Zhou, L. Xing, S. Wang, M. Ho, Z. Peng, Y. T. Tai, T. Hideshima, K. C. Anderson, Y. Cang, *Leukemia* **2019**, *33*, 171-180.
[21] A. Patil, M. Manzano, E. Gottwein, *Blood Adv* **2019**, *3*, 2105-2117.
[22] K. M. Reichermeier, R. Straube, J. M. Reitsma, M. J. Sweredoski, C. M. Rose, A. Moradian, W. den Besten, T. Hinkle, E. Verschueren, G. Petzold, N. H. Thoma, I. E. Wertz, R. J. Deshaies, D. S. Kirkpatrick, *Mol Cell* **2020**, *77*, 1092-1106 e1099.
[23] S. Tateno, M. Iida, S. Fujii, T. Suwa, M. Katayama, H. Tokuyama, J. Yamamoto, T. Ito, S. Sakamoto, H. Handa, Y. Yamaguchi, *Sci Rep* **2020**, *10*, 4012.
[24] R. Shirasaki, G. M. Matthews, S. Gandolfi, R. de Matos Simoes, D. L. Buckley, J. Raja Vora, Q. L. Sievers, J. B. Bruggenthies, O. Dashevsky, H. Poarch, H. Tang, M. A. Bariteau, M. Sheffer, Y. Hu, S. L. Downey-Kopyscinski, P. J. Hengeveld, B. J. Glassner, E. Dhimolea, C. J. Ott, T. Zhang, N. P. Kwiatkowski, J. P. Laubach, R. L. Schlossman, P. G. Richardson, A. C. Culhane, R. W. J. Groen, E. S. Fischer, F. Vazquez, A. Tsherniak, W. C. Hahn, J. Levy, D. Auclair, J. D. Licht, J. J. Keats, L. H. Boise, B. L. Ebert, J. E. Bradner, N. S. Gray, C. S. Mitsiades, *Cell Rep* **2021**, *34*, 108532.
[25] C. Surka, L. Jin, N. Mbong, C. C. Lu, I. S. Jang, E. Rychak, D. Mendy, T. Clayton, E. Tindall, C. Hsu, C. Fontanillo, E. Tran, A. Contreras, S. W. K. Ng, M. Matyskiela, K. Wang, P. Chamberlain, B. Cathers, J. Carmichael, J. Hansen, J. C. Y. Wang, M. D. Minden, J. Fan, D. W. Pierce, M. Pourdehnad, M. Rolfe, A. Lopez-Girona, J. E. Dick, G. Lu, *Blood* **2021**, *137*, 661-677.
[26] N. S. Scholes, C. Mayor-Ruiz, G. E. Winter, *Cell Chem Biol* **2021**, *28*, 1048-1060.
[27] A. Hanzl, R. Casement, H. Imrichova, S. J. Hughes, E. Barone, A. Testa, S. Bauer, J. Wright, M. Brand, A. Ciulli, G. E. Winter, *Nat Chem Biol* **2023**, *19*, 323-333.
[28] B. Jiang, Y. Gao, J. Che, W. Lu, I. H. Kaltheuner, R. Dries, M. Kalocsay, M. J. Berberich, J. Jiang, I. You, N. Kwiatkowski, K. M. Riching, D. L. Daniels, P. K. Sorger, M. Geyer, T. Zhang, N. S. Gray, *Nat Chem Biol* **2021**, *17*, 675-683.
[29] P. M. Gosavi, K. C. Ngan, M. J. R. Yeo, C. Su, J. Li, N. Z. Lue, S. M. Hoenig, B. B. Liau, *ACS Cent Sci* **2022**, *8*, 417-429.
[30] C. Mayor-Ruiz, S. Bauer, M. Brand, Z. Kozicka, M. Siklos, H. Imrichova, I. H. Kaltheuner, E. Hahn, K. Seiler, A. Koren, G. Petzold, M. Fellner, C. Bock, A. C. Muller, J. Zuber, M. Geyer, N. H. Thoma, S. Kubicek, G. E. Winter, *Nat Chem Biol* **2020**, *16*, 1199-1207.
[31] D. Ross, D. Siegel, *Redox Biol* **2021**, *41*, 101950.
[32] E. T. Oh, H. J. Park, *BMB Rep* **2015**, *48*, 609-617.
[33] G. Ahn, N. M. Riley, R. A. Kamber, S. Wisnovsky, S. Moncayo von Hase, M. C. Bassik, S. M. Banik, C. R. Bertozzi, *Science* **2023**, *382*, eadf6249.
[34] S. Hosoda, W. Nakamura, K. Hayashi, *J Biol Chem* **1974**, *249*, 6416-6423.
[35] M. Faig, M. A. Bianchet, P. Talalay, S. Chen, S. Winski, D. Ross, L. M. Amzel, *Proc Natl Acad Sci U S A* **2000**, *97*, 3177-3182.
[36] G. Asher, O. Dym, P. Tsvetkov, J. Adler, Y. Shaul, *Biochem* **2006**, *45*, 6372-6378.
[37] S. L. Winski, M. Faig, M. A. Bianchet, D. Siegel, E. Swann, K. Fung, M. W. Duncan, C. J. Moody, L. M. Amzel, D. Ross, *Biochem* **2001**, *40*, 15135-15142.
[38] L. S. M. Pidugu, J. C. E. Mbimba, M. Ahmad, E. Pozharski, E. A. Sausville, A. Emadi, E. A. Toth, *BMC Struct Biol* **2016**, *16*, 1.
[39] S. Cuff, R. D. Lewis, E. Chinje, M. Jaffar, R. Knox, I. Weeks, *Free Radic Biol Med* **2018**, *116*, 141-148.
[40] R. M. Meyers, J. G. Bryan, J. M. McFarland, B. A. Weir, A. E. Sizemore, H. Xu, N. V. Dharia, P. G. Montgomery, G. S. Cowley, S. Pantel, A. Goodale, Y. Lee, L. D. Ali, G. Jiang, R. Lubonja, W. F. Harrington, M. Strickland, T. Wu, D. C. Hawes, V. A. Zhivich, M. R. Wyatt, Z. Kalani, J. J. Chang, M. Okamoto, K. Stegmaier, T. R. Golub, J. S. Boehm, F. Vazquez, D. E. Root, W. C. Hahn, A. Tsherniak, *Nat Genet* **2017**, *49*, 1779-1784.
[41] A. Tsherniak, F. Vazquez, P. G. Montgomery, B. A. Weir, G. Kryukov, G. S. Cowley, S. Gill, W. F. Harrington, S. Pantel, J. M. Krill-Burger, R. M. Meyers, L. Ali, A. Goodale, Y. Lee, G.

Jiang, J. Hsiao, W. F. J. Gerath, S. Howell, E. Merkel, M. Ghandi, L. A. Garraway, D. E. Root, T. R. Golub, J. S. Boehm, W. C. Hahn, *Cell* **2017**, *170*, 564-576 e516.
[42] D. Menon, A. Innes, A. J. Oakley, J. E. Dahlstrom, L. M. Jensen, A. Brustle, P. Tummala, M. Rooke, M. G. Casarotto, J. B. Baell, N. Nguyen, Y. Xie, M. Cuellar, J. Strasser, J. L. Dahlin, M. A. Walters, G. Burgio, L. A. J. O'Neill, P. G. Board, *Sci Rep* **2017**, *7*, 17832.
[43] C. R. Huang, T. W. Chang, C. T. Lee, C. J. Shen, W. C. Chang, B. K. Chen, *Oncogenesis* **2021**, *10*, 11.
[44] D. Lang, S. I. Schulz, I. Piel, D. T. Tshitenge, H. Stass, *Chem Res Toxicol* **2022**, *35*, 2037-2048.
[45] C. A. Ramsden, V. Milata, in *Advances in Heterocyclic Chemistry, Vol. 92* (Ed.: A. R. Katritzky), Academic Press, **2006**, pp. 1-54.
[46] C. Plaçais, M. Donnard, A. Panossian, J.-P. Vors, D. Bernier, S. Pazenok, F. R. Leroux, *Organic Letters* **2021**, *23*, 4915-4919.
[47] A. Ryan, E. Kaplan, N. Laurieri, E. Lowe, E. Sim, *Scientific Reports* **2011**, *1*, 63.
[48] N. H. Zuma, J. Aucamp, D. D. N'Da, *Eur J Pharm Sci* **2019**, *140*, 105092.
[49] H. Li, Z. Zhang, X. Yang, X. Mao, Y. Wang, J. Wang, Y. Peng, J. Zheng, *Chem Res Toxicol* **2019**, *32*, 681-690.
[50] J. Yu, D. E. Mathisen, D. Burdette, D. G. Brown, C. Becker, D. Aharony, *Drug Metab Dispos* **2010**, *38*, 46-60.
[51] D. Ross, J. K. Kepa, S. L. Winski, H. D. Beall, A. Anwar, D. Siegel, *Chem-Biol Interact* **2000**, *129*, 77-97.
[52] A. Kobayashi, M. I. Kang, H. Okawa, M. Ohtsuji, Y. Zenke, T. Chiba, K. Igarashi, M. Yamamoto, *Mol Cell Biol* **2004**, *24*, 7130-7139.
[53] R. J. Riley, P. Workman, *Biochem Pharmacol* **1992**, *43*, 1657-1669.
[54] Y. Yang, Y. Zhang, Q. Wu, X. Cui, Z. Lin, S. Liu, L. Chen, *J Exp Clin Cancer Res* **2014**, *33*, 14.
[55] D. Ross, D. Siegel, H. Beall, A. S. Prakash, R. T. Mulcahy, N. W. Gibson, *Cancer Metastasis Rev* **1993**, *12*, 83-101.
[56] K. Lei, X. Gu, A. G. Alvarado, Y. Du, S. Luo, E. H. Ahn, S. S. Kang, B. Ji, X. Liu, H. Mao, H. Fu, H. I. Kornblum, L. Jin, H. Li, K. Ye, *J Hematol Oncol* **2020**, *13*, 141.
[57] K. A. Nolan, J. R. Doncaster, M. S. Dunstan, K. A. Scott, A. D. Frenkel, D. Siegel, D. Ross, J. Barnes, C. Levy, D. Leys, R. C. Whitehead, I. J. Stratford, R. A. Bryce, *J Med Chem* **2009**, *52*, 7142-7156.
[58] T. A. Giovannucci, F. A. Salomons, M. Haraldsson, L. H. M. Elfman, M. Wickström, P. Young, T. Lundbäck, J. Eirich, M. Altun, R. Jafari, A.-L. Gustavsson, J. I. Johnsen, N. P. Dantuma, *Cell Death Dis* **2021**, *12*, 914.
[59] F. D. Johnson, J. Ferrarone, A. Liu, C. Brandstadter, R. Munuganti, D. A. Farnsworth, D. Lu, J. Luu, T. Sihota, S. Jansen, A. Nagelberg, R. Shi, G. C. Forcina, X. Zhang, G. S. W. Cheng, S. E. Spencer Miko, G. de Rappard-Yuswack, P. H. Sorensen, S. J. Dixon, U. Guha, K. Becker, H. Djaballah, R. Somwar, H. Varmus, G. B. Morin, W. W. Lockwood, *Cell Rep* **2022**, *38*, 110343.
[60] D. Siegel, C. Yan, D. Ross, *Biochem Pharmacol* **2012**, *83*, 1033-1040.
[61] G. M. Dal Forno, E. Latocheski, A. Beatriz Machado, J. Becher, L. Dunsmore, A. L. St. John, B. L. Oliveira, C. D. Navo, G. Jiménez-Osés, R. Fior, J. B. Domingos, G. J. L. Bernardes, *J Am Chem Soc* **2023**, *145*, 10790-10799.
[62] H. D. Beall, A. M. Murphy, D. Siegel, R. H. Hargreaves, J. Butler, D. Ross, *Mol Pharmacol* **1995**, *48*, 499-504.

10.1002/anie.202316730

## TABLE OF CONTENTS

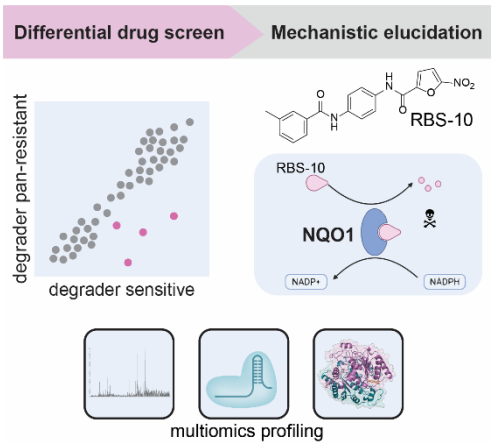


The small molecule RBS-10 exploits a novel synthetic lethal vulnerability in cancer cells that show widespread resistance to degraders.

**Twitter handles**: @CrisMayorRuiz @IRBBarcelona @BarbMGBarbosa @KarenSfyaki